ORIGINAL ARTICLE

SAR Performance for Breast Cancer Hyperthermia Treatment using 2.45GHz and 0.915GHz Circular Non-Invasive Microstrip Patch Antenna integrated with Various Shapes of Water Boluses

Mazlina Mansor Hassan[1,2], Kasumawati Lias[1], Norlida Buniyamin[3], Ahmad Tirmizi Jobli[4], Bibi Sarpinah Sheikh Naimullah[1,2], Dzufi Iszura Ispawi[2]

[1] Department of Electrical and Electronics Engineering, Faculty of Engineering, Universiti Malaysia Sarawak, 94300 UNIMAS Kota Samarahan, Sarawak, Malaysia
[2] Electrical Engineering Studies, College of Engineering, Universiti Teknologi MARA, 94300 UiTM Kota Samarahan, Sarawak, Malaysia
[3] Electrical Engineering Studies, College of Engineering, Universiti Teknologi MARA, 40450 UiTM Shah Alam, Selangor, Malaysia
[4] Faculty of Medicine and Health Sciences, Universiti Malaysia Sarawak, 94300 UNIMAS Kota Samarahan, Sarawak Malaysia

ABSTRACT

Introduction: This research presents a hyperthermia treatment procedure using a circular microstrip patch antenna integrated with a water bolus to destroy malignant tissues. Hyperthermia uses high temperatures from 41℃ to 45℃ to denaturate cancer tissues into necrotic tissues. However, there are some limitations in hyperthermia treatment such as limited penetration depth, poor focus position distance and significant undesired heating. Therefore, the research is carried out to enhance the limitations above especially when it is used alone and not adjuvant with other conventional therapies such as chemotherapy and radiotherapy. **Materials and methods:** SEMCAD X 14.8.4 is used as a software simulator to develop antenna, breast phantom, cancer cells and water boluses. Three cancer tissue diameters are considered in the research, which are 15 mm, 34 mm and 59 mm, based on analysis of the mammogram images received from the referred Hospital. A 2.45 GHz and 0.915 GHz antennas were used as the operating frequency in the research to destroy the malignant tissues. Different shapes of water boluses and liquids of deionized and distilled water boluses integrated with the antenna to reduce the unwanted hotspots and maintain the focus position distance. Hyperthermia has some advantages such as it can be non-invasive and provide less adverse health effects. **Results:** Water boluses of different shapes and antenna frequencies provide sufficient focus position distance, penetration depth and estimation times during the execution of the hyperthermia treatment. **Conclusion:** The various shapes of the water bolus provide adequate heat to the T1, T2 and T3 malignant tissues while minimizing the presence of undesirable hotspots.
Malaysian Journal of Medicine and Health Sciences (2025) 21(SUPP11): 108-116. doi:10.47836/mjmhs.21.s11.16

Keywords: Hyperthermia, Circular microstrip patch antenna, Water bolus, Focus position distance, Unwanted hotspots

Corresponding Author:
Mazlina Mansor Hassan, PhD
Email: mazlina2206@gmail.com
Tel : +60-138201089

INTRODUCTION

Breast cancer is a crucial disease affecting women globally. A report from the World Health Organization (WHO) shows that breast cancer incidence rate and fatality rate due to the illness rise every year. Statistics from WHO show that people diagnosed with breast cancer were 2 million in 2018, and the number increase to 2.3 million in 2022 (1,2). Breast cancer is reported as the first or second leading cause of mortality rate, and WHO statistics report confirms that 6.3 million patients died due to the illness in 2018, and the number increased to 6.65 million in 2022 respectively (1-3).

Hyperthermia uses high heat, where the temperature is elevated from 41℃ to 45℃ , to denaturate cancer tissues into necrotic tissues (4,5). It is also known as a thermal therapy to shrink and destroy malignant tissues. Hyperthermia has been used as an alternative treatment for breast cancer. It provides less adverse health effects than conventional cancer treatment (6). Hyperthermia can be invasive, where the probe of the applicator is inserted into the patient's body, such as interstitial and intracavitary techniques (5) or non-invasive, where the applicator is placed outside of the patient body. Hyperthermia can be used alone or in adjuvant with other conventional cancer techniques to improve the treatment (7,8). Hyperthermia can be used in conjunction with chemotherapy to enhance the chemical reactions within the patient's body (9,10). Furthermore, it can be used with radiotherapy to expedite the radiation procedure (9,5). The combination

of hyperthermia treatment reduces the size of the malignant tissues before surgery is done. Hyperthermia is able to eradicate any microscopic malignant tissues that are not visible to the naked eye since it delivers heat to the targeted region. Nevertheless, hyperthermia has several limitations, such as poor focus position distance, low penetration depth and the creation of unwanted hotspots in the breast phantom especially when non-invasive hyperthermia is carried out (11). Hence, the research is carried out to enhance the limitation such as to improve the focus position distance, penetration depth and reduce unwanted hotspots in the breast phantom. The research involves manipulating several variables including antenna frequency, antenna position with and without a water bolus, the shape of the water bolus and type of liquid used in the water bolus.

A circular microstrip patch antenna is used as the applicator to deliver heat to the malignant tissues in the hyperthermia treatment. The microstrip patch antenna was selected because of its advantageous features it has such as lightweight, low cost, easy to manufacture and small size, which make it well suited to be used in the research (12,13). The antenna utilizes Rogers Duroid, RT5880. The substrate has a permittivity of 2.2 and a thickness of 1.575 mm. Previous research has shown that RT5880 show good SAR distribution in the treated regions (14). A 2.45 GHz and 0.915 GHz antennas are used in the research, and it is the Industrial, Scientific and Medical (ISM) frequency for hyperthermia applications, and it is used together with various shapes of water boluses. Three malignant tissues are used in the research with diameter sizes of 15 mm, 34 mm and 59 mm and labelled as T1, T2 and T3. Water bolus is a cooling element used to cool the treated skin surface and can improve the coupling effects of the antenna and breast phantom (15). A 2 mm thickness of distilled water (DI) and deionized water (DS) is used as the water bolus (WB) in the research, and their performance is compared. The antenna is the main element in hyperthermia treatment to kill the malignant tissues, whereas the coupling of the water boluses with the antenna helps to distribute the heat to the target region, reduce unwanted hotspots and maintain the focus position distance (FPD) (16). Focus position distance involved several factors such as, analysis of the mammogram images, desired penetration depth and focus of the heat distribution. Surface depth and Inner depth were measured from DICOM software, and average surface depth and average inner depth were calculated for 72 mammogram images. Focus position distance is the average range of surface depth and inner depth. The focus position distance is required to get optimal distance for focusing the energy.

MATERIALS AND METHODS

Methodology

The methodology is divided into three sections, which include the initial phase for breast phantom and malignant tissues, the design of experiment 1 (DoE 1): antenna development and the design of experiment 2 (DoE 2): water bolus development. DoE 1 focus on development of antennas using two different frequencies. A more detailed explanation of the methodology is discussed in the following sections.

Initial Phase

The ethical letter was obtained from the referred Hospital before conducting the research. A total of 72 mammogram images were received from the referred Hospital. The 113 mm diameter size of the breast phantom is used in the research. Mammogram images are analysed using RadiAnt Digital Imaging and Communication in Medicine (DICOM) software to get the penetration depth and focus position distance (FPD). Surface depth and inner depth are calculated to get the average diameter size of the malignant tissues. Malignant tissues are categorized into three sizes, which are 15 mm, 34 mm and 59 mm and are labelled as T1, T2 and T3, respectively. The sizes of the malignant tissues are determined from the location and depth of the malignant tissues. The sizes are based on tumour standard size where T1<=20 mm, 20 mm < T2 <=50 mm and T3>50 mm. The focus position distance, FPD, ranges from 57 mm to 64 mm, 39 mm to 88 mm and 34 mm to 95m for each size of malignant tissues T1, T2 and T3, respectively. The ground-thru process carried out with the radiologist to confirm the malignant tissue measurements.

Table I shows the breast phantom and malignant tissue's electro-thermal properties. The formula in Eq. (1) is used to determine the average surface depth. Eq. (2) is, on the other hand, used to compute the average inner depth, and Eq. (3) was used to calculate the size of malignant tissues. The mediolateral Oblique (MLO) is the angle view of 450 to 600 of the above position of the breast phantom while the cranio-caudal is the top-down view from above of the breast phantom (7). Fig.1 shows the arrangements set up for the experiments, fabricated 0.915 GHz and 2.45 GHz antennas with their return loss respectively. Both return loss of 0.915 GHz and 2.45 GHz fabricated antennas produced 10.168 dB and 10.8667 dB respectively. Return loss below 10 dB signifies a good impedance match between the antenna and the transmission line.

$$= \frac{MLO_{(S)} + CC_{(S)}}{2} \quad (1)$$

$$= \frac{MLO_{(I)} + CC_{(I)}}{2} \quad (2)$$

$$Size\ of\ Cancer\ Cell = Av_I - Av_S \quad (3)$$

Table I: Electro-Thermal Properties

Tissue	Relative permittivity	Electrical Conductivity (s/m)	Density (mm)	Diameter (mm)	Specific Heat Capacity (J/Kg/K)
Breast Fat	5.14	0.125	911	113	3060
Cancer T1	28.0259	16.232	1000	15	3060
Cancer T2	43.233	4.838	1000	34	3060
Cancer T3	14.741	1.026	1000	59	3060

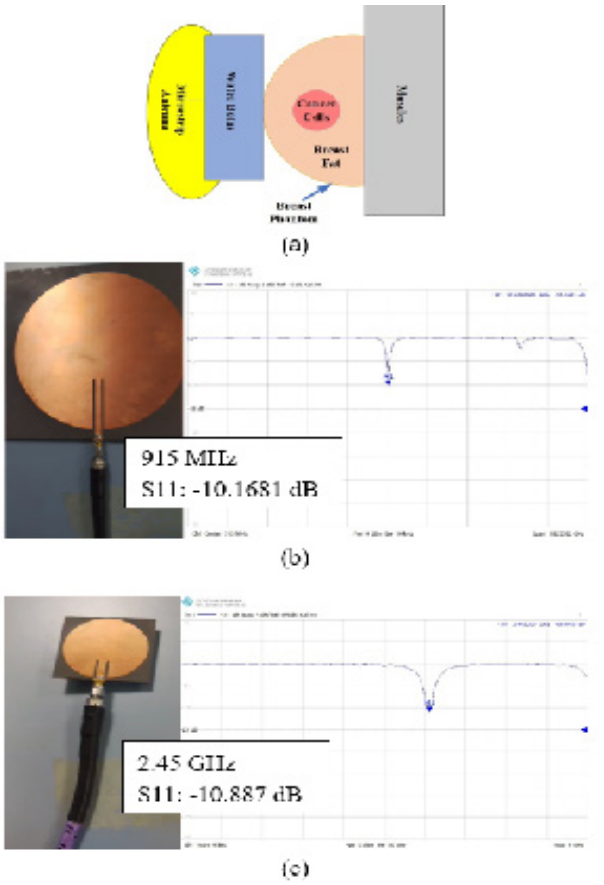

Fig. 1: Experiment setup, fabricated antennas and return loss. Figure 1(a) The arrangements set-up for the experiment. Circular microstrip patch antenna was developed in this research. Figure 1(b) and Figure 1(c) shows two fabricated antennas were developed to destroy T1, T2 and T3 malignant tissues with return loss results. Antenna is integrated with various shapes of water boluses. Water bolus indicated by blue color and malignant tissues indicated by red color.

The Average Surface Depth, denoted as Avs and Average Inner depth, denoted as AvI and measure in mm. Medio-Lateral Oblique (MLO) and Cranio-Caudal (CC) are two standard views used in mammography screening. MLO is the breast phantom image taken at a standard angle of 45℃ and the angle can be varied from 40℃ to 60℃ to get the best view of the mammogram images. Meanwhile CC is the top-down view of the breast phantom. Both MLO and CC measurement of surface depth and inner depth of the malignant cells in each breast phantom is analysed for total the of 72 mammogram images received from Hospital. Then average surface depth and average inner depth of the malignant cells were calculated using Eq. (1) and Eq. (2) respectively. Average surface depth is the sum of medio-lateral oblique surface depth and cranio-caudal surface depth divided by 2. Meanwhile average inner depth is the sum of mediolateral oblique inner depth and cranio-caudal inner depth divided by 2. Meanwhile, Eq. (3) is the formula used to calculate the sizes of malignant cells which is the different of Eq. (2) and Eq. (1).

Design of Experiment 1: Antenna Development

A circular microstrip patch antenna is designed with an inset feed line and operated at 2.45 GHz and 0.915 GHz frequency bands. Rogers Duroid, RT5880, with permittivity of 2.2 and thickness of 1.575 mm, is used as a dielectric of the antenna. Antenna setups are as shown in Fig. 1. The length and width of 0.915 GHz antenna substrate are 144.92 mm and 147.92 mm respectively with 64.62 mm radius of circular patch. Meanwhile the length and width of 2.45 GHz antenna substrate are 53.818 mm and 51.327 mm respectively with 24.34 mm radius of circular patch. The antenna is initially placed directly to the breast phantom before it is integrated with four different shapes of water bolus. Fig. 1(a) shows the antenna and water bolus arrangement for the experiment, whereas Fig. 1(b) and Fig. 1(c) shows fabricated 0.915 GHz and 2.45 GHz antennas with the return loss. Their performance are compared and recorded in Table II and Table III. Antenna parameters are calculated using Eq. (6) to Eq. (11) as follows:

$$\text{Width of Substrate and Ground, Width, } W = \frac{C}{2C\sqrt{\frac{\varepsilon_r + 1}{2}}} \quad (6)$$

$$\text{Effective Dielectric Constant, } \varepsilon_{ff} = \frac{\varepsilon_r + 1}{2} + \frac{\varepsilon_r + 1}{2}\left(1 + 12\frac{W}{h}\right)^{0.5} \quad (7)$$

$$\text{Length Extension, } \Delta L = 0.412h \frac{(\varepsilon_{eff}+0.3)\left(\frac{W}{h}+0.264\right)}{(\varepsilon_{eff}+0.258)\left(\frac{W}{h}+0.8\right)} \quad (8)$$

$$\text{Effective Length, } L_{eff} = \frac{C}{2f_r\sqrt{\varepsilon_{eff}}} \quad (9)$$

$$\textit{Actual Length, } \Delta L = L_{eff} - 2\Delta L \quad (10)$$

$$\text{Radius of Circular Patch, } \alpha = \frac{F}{\sqrt{1+\frac{2h}{f\pi\varepsilon_r}\left[\ln\ln\left(\frac{\pi f}{2h}\right)+1.7726\right]}} = \frac{8.791 \times 10^9}{f_r\sqrt{\varepsilon_r}} \quad (11)$$

The parameters for designing the circular antenna include ε_r, which presents the permittivity of the dielectric, w and h, which indicate the width and the height of the substrate, respectively. The radius of the circular patch is labelled as a. Other variables involved are the speed of light, denoted as C, and the resonant frequency indicated as f_r.

Specific absorption rate (SAR) refers to the rate at which the mass of body tissues absorbs heat, and it is expressed in W/Kg or mw/g (17). The calculation can be performed using the formulas listed in Eq. (4) and Eq. (5) as follows (18):

$$= \frac{\sigma}{2\,||\,E\,||^2} = \rho.(SAR) \quad (4)$$

$$= \frac{C\Delta T}{\Delta t} \quad (5)$$

The variables listed in Eq. (4) and Eq. (5) are Electrical conductivity E, which is expressed in (Sm-1), Tissue density, ρ is in (kg m-3), Specific Heat Capacity of tissue, C is expressed in (J-1kg °C), and Primary time derivative of tissue temperature, computed using this formula (ΔT/Δt) where ΔT represents temperature rise in Celsius and t is the exposure time in seconds (7).

Table II: Sample of SAR results using Applicator with and without Water Boluses

No Water Bolus		
Applicator T1	**Applicator T2**	**Applicator T3**
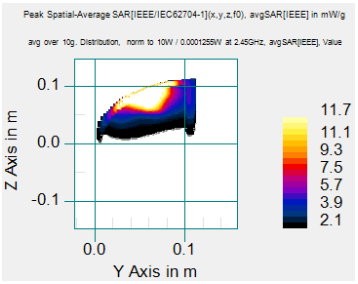	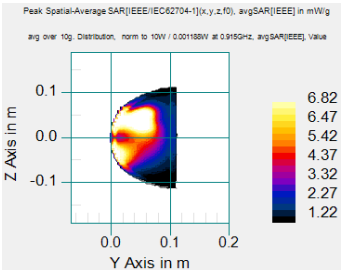	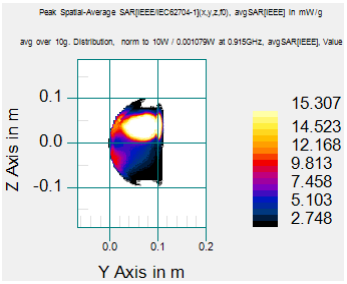
SAR: 11.70 mW/g Times: 0.58 hours FPD: 26 mm - 80 mm	SAR: 6.82 mW/g Time: 1 hours FPD: 38 mm – 71 mm	SAR: 15.31 mW/g Time: 0.44 hours FPD: 28 mm – 108 mm
Antenna with Water Bolus (Deionized Water)		
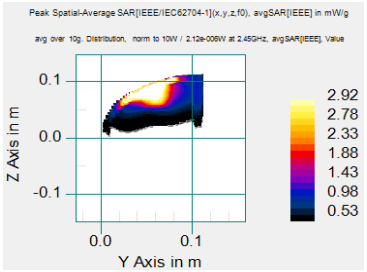	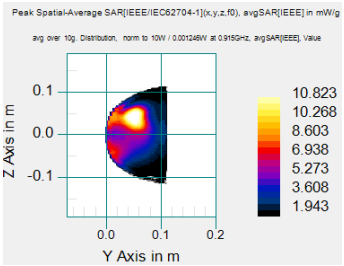	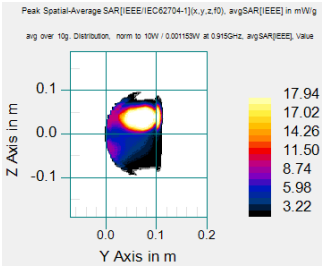
SAR: 2.92 mW/g Time: 2.33 hours FPD: 23 mm – 73 mm Rectangular Shape	**SAR: 10.82 mW/g** **Time: 0.63 hours** **FPD: 36 mm – 73 mm** **Cone Shape**	SAR: 17.94 mW/g Time: 0.38 hours FPD: 35 mm – 107 mm Circular Shape

CONTINUE

Table II: Sample of SAR results using Applicator with and without Water Boluses (CONT.)

Antenna with Water Bolus (Distilled Water)		
Applicator T1	**Applicator T2**	**Applicator T3**
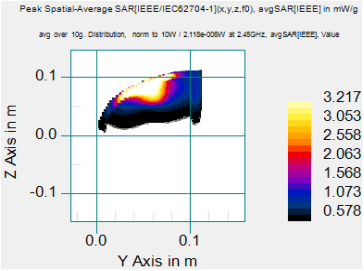	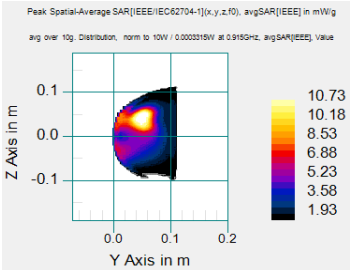	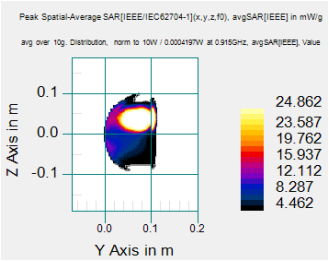
SAR: 3.22 mW/g Time: 2.11 hours FPD: 25 mm – 80 mm Circular Shape	SAR: 10.73 mW/g Time: 0.63 hours FPD: 32 mm – 68 mm Rectangular Shape	SAR: 24.86 mW/g Time: 0.27 hours FPD: 34 mm – 108 mm Rectangular Shape

Table III: SAR for Applicator using Various Shapes of Water Boluses

	Applicator T1 and Water Bolus (DI)			
No	**Rectangular**	**Circular**	**Sphere**	**Cone**
1.	SAR: 2.92 mW/g Time: 2.33 hours FPD: 23 mm – 73 mm	SAR: 2.73 mW/g Time: 2.49 hours FPD: 23 mm – 70 mm	SAR: 2.14 mW/g Time: 3.18 hours FPD: 22 mm – 66 mm	SAR: 2.34 mW/g Time: 2.91 hours FPD: 22 mm – 67 mm
	Applicator T2 and Water Bolus (DI)			
2.	SAR: 5.80 mW/g Time: 1.17 hours FPD: 36 mm – 71 mm	SAR: 6.05 mW/g Time: 1.12 hours FPD: 36 mm– 73 mm	SAR: 10.73 mW/g Time: 0.63 hours FPD: 31 mm – 67 mm	SAR: 10.82 mW/g Time: 0.63 hours FPD: 36 mm – 73 mm
	Applicator T3 and Water Bolus (DI)			
3.	SAR: 67.96 mW/g Time: 0.10 hours FPD: 36 mm – 71 mm	SAR: 17.94 mW/g Time: 0.38 hours FPD: 35 mm – 107 mm	SAR: 18.62 mW/g Time: 0.37 hours FPD: 35 mm– 105 mm	SAR: 17.94 mW/g Time: 0.38 hours FPD: 36 mm– 107 mm
	Applicator T1 and Water Bolus (DS)			
4.	SAR: 2.44 mW/g Time: 2.78 hours FPD: 23 mm – 73 mm	SAR: 3.22 mW/g Time: 2.11 hours FPD: 25 mm – 80 mm	SAR: 2.73 mW/g Time: 2.49 hours FPD: 23 mm – 68 mm	SAR: 2.73 mW/g Time: 2.49 hours FPD: 23 mm – 70 mm
	Applicator T2 and Water Bolus (DS)			
5.	SAR: 10.73 mW/g Time: 0.63 hours FPD: 32 mm – 68 mm	SAR: 10.73 mW/g Time: 0.63 hours FPD: 32 mm – 68 mm	SAR: 10.73 mW/g Time: 0.63 hours FPD: 31 mm – 67 mm	SAR: 10.82 mW/g Time: 0.63 hours FPD: 36 mm– 73 mm
	Applicator T3 and Water Bolus (DS)			
6.	SAR: 24.86 mW/g Time: 0.27 hours FPD: 34 mm – 108 mm	SAR: 17.65 mW/g Time: 0.39 hours FPD: 35 mm– 107 mm	SAR: 18.04 mW/g Time: 0.38 hours FPD: 37 mm – 106 mm	SAR: 18.14 mW/g Time: 0.38 hours FPD: 36 mm– 106 mm

Design of Experiment 2: Water Bolus

The SEMCAD X 14.8.4 software simulator is used to develop four different shapes of water boluses such as rectangular, circular, sphere and cone. The circular microstrip patch antenna is connected with a 2 mm thickness of distilled and deionized water boluses, which is then attached on the surface of the breast phantom. The water bolus serves as a coolant for the skin surface and enhances the dispersion of heat in the breast phantom. Initially the 2.415 GHz and 0.915 GHz circular microstrip patch antenna positioned directly on the breast phantom without water bolus to heat T1, T2 and T3 malignant tissues. The following experiment was integrating antenna with modified structures of various shapes of water boluses. Integration of antennas with water boluses aims to deliver heat to the target region to destroy the malignant tissues.

Ethical Clearance

The Medical Research and Ethics Committee (MREC), Ministry of Health (MOH) has provided ethical approval for this study, Ref: KKM/NIHSEC/P20-578(12).

RESULTS

Return loss, S_{11} and Radiation Pattern of Circular Microstrip Patch Antenna

Return loss S_{11}, of the 2.45 GHz is 14.82 dB. The antenna is developed to destroy T1 malignant tissues. The input Impedance is 50 ohms to reduce impedance mismatch or signal loss between the patch and the feed line. Meanwhile, return loss for 0.915 GHz is 12.916 dB. The antenna is developed to destroy T2 and T3 malignant tissues. Both 2.45 GHz and 0.915 GHz antennas met the requirement for signal transmission with a return loss less than 10 dB. Meanwhile, fabricated 0.915 GHz and 2.45 GHz antennas presented slightly different value of return loss. But all the return loss results from fabricated antennas produced below 10 dB which indicate a good match between antenna and the transmission lines. A

2.45 GHz shows higher return loss than 0.915 GHz. The simulation results for both antennas agree with return loss result from fabricated antennas. A 0.915 GHz antenna is able to destroy T2 and T3 sizes of malignant tissues, whereas a modification position of a 2.45 GHz antenna enables the applicator to eradicate T1 malignant tissues.

Directional antenna is used in the research. The polar plot radiation of 2.45 GHz for E-plane and H-plane main lobe directivity is at 4 degree and 0 degree respectively. Meanwhile, for antenna operate at 0.915 GHz the polar plot radiation E-plane and H-plane main lobe directivity is at 1 degree and 0 degree respectively.

Specific Absorption Rate (SAR)

In Table II, antenna with no water bolus in the first row shows the specific absorption rate (SAR) results when the antenna is positioned in close proximity to the breast phantom. The breast phantom receives a significant increase in temperature, particularly in T1 and T2 malignant tissues. The lowest SAR results were indicated by T2 with 6.82 mW/g, followed by T1 with 11.7 mW/g and T3 with 15.31 mW/g. A lower SAR value shows higher temperatures generated within the breast model. The estimated time to destroy the malignant tissues for circular antenna without water bolus is around 0.58 hours, 1 hour and 0.44 hours for T1, T2 and T3 sizes of malignant tissues, respectively.

In the same Table II, in the second row shows sample of best SAR results for T1, T2 and T3 when antenna is integrated with 2 mm deionized water bolus. Meanwhile Table II in the third row shows sample of best SAR results for T1, T2 and T3 when antenna was integrated with 2 mm distilled water bolus. Table III shows reading for all SAR using circular antenna integrated with various shapes of water boluses.

The graphs in Fig.2, Fig.3 and Fig.4 show the required surface depth and the required inner depth for T1, T2 and T3 applicators to destroy the malignant tissues. The required surface depth is indicated with a dark green line, while the required inner depth is indicated with light green line. The figures, namely Fig.2, Fig.3, and Fig.4 depict different shapes of distilled and deionized water bolus. The surface depth of rectangular, circular, sphere and cone shapes of distilled water are represented in a light purple. Meanwhile, the inner depth of the different shapes of distilled water bolus is highlighted in a light blue. An orange colour indicates the surface depth of deionized water bolus with different shapes, while a dark purple represents the inner depth of deionized water.

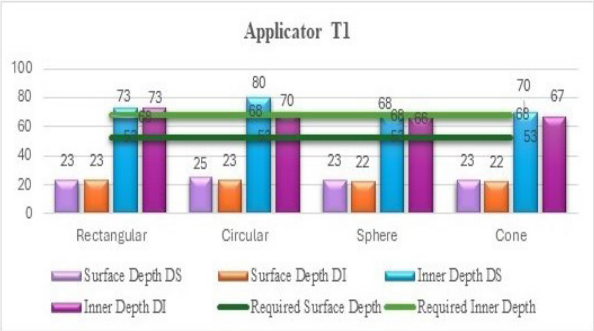

Fig. 2: Surface depth and Inner depth presented for Applicator T1. Results of an applicator T1, a 2.45 GHz antenna paired with various shapes of water bolus and placed on the surface of the breast phantom. Some modifications for the antenna are made to deliver heat to the malignant tissues. The modifications include some changes, such as the position of the antenna was reversed, the antenna moving 80 mm to the upper part of the breast phantom, and placed 45 from the breast phantom. The modification enables heat to move towards the malignant tissues. The required surface depth and inner depth for TI malignant tissues are 53 mm and 68 mm, respectively. The graph shows that all shapes of water boluses meet the required surface depth and inner depth of T1 malignant tissues except for cone water boluses, which almost achieve the inner depth of 68 mm. However, the applicator for T1 creates significant undesired heating, as in Table 3, especially at the front side of the breast phantom. Excessive heat can also be seen in Fig.3, where the heat is produced at 22 mm, 23 mm and 25 mm from the required surface depth of 53 mm.

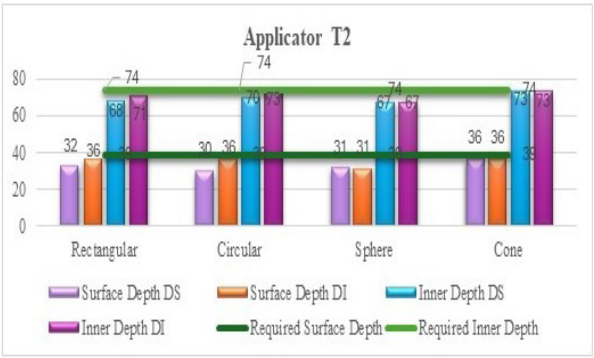

Fig. 3: Surface depth and Inner depth presented for Applicator T2. The average surface depth, and the average inner depth of heat delivered to malignant tissues using applicator T2. A 0.915 GHz antenna is coupled with various shapes of water bolus such as rectangular, circular, sphere and cone shapes, and it is placed on the surface of the breast phantom. The required surface depth and inner depth for T2 malignant tissues are 39 mm and 74 mm, respectively. The graph shows that all shapes of water boluses meet the required surface depth of T2 malignant tissues. However, for average inner depth, all shapes of water boluses approximately reached the required depth, which is 74 mm. 73 mm depth is the nearest to the inner depth necessary achieved using applicator T2 by employing circular shapes of deionized water bolus as well as a cone shape of distilled and deionized water bolus.

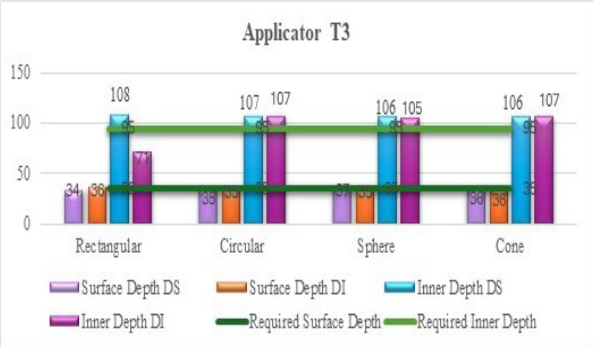

Fig. 4: Surface depth and Inner depth presented for Applicator T3. The average surface depth and average inner depth of heat delivered to T3 malignant tissues is as shown in the graph. A 0.915 GHz antenna was coupled with various shapes of water bolus and able to destroy T3 malignant tissues. The required surface depth and inner depth for T3 malignant tissues are 35 mm and 95 mm, respectively. The graph shows that all shapes of water boluses achieved the required surface depth of T3 malignant tissues. However, for average inner depth, all shapes of water boluses reached the required inner depth, except the antenna with rectangular water bolus does not meet the required inner depth.

The graph in Fig.2 shows that all shapes and type of water boluses meet the required surface depth and inner depth of T1 malignant tissues except for cone water bolus, which almost achieve the inner depth of 68 mm.

Fig.3 shows the average surface depth, and the average inner depth of heat delivered to malignant tissues using applicator T2. A 0.915 GHz antenna is coupled with various shapes of water bolus such as rectangular, circular, sphere and cone shapes, and it is placed on the surface of the breast phantom. The required surface depth and inner depth for T2 malignant tissues are 39 mm and 74 mm, respectively. The graph shows that all shapes of water boluses meet the required surface depth of T2 malignant tissues. However, for average inner depth, all shapes of water boluses approximately reached the required depth, which is 74 mm. 73 mm depth is the nearest to the inner depth achieved using applicator T2 by employing circular shapes of deionized water bolus as well as a cone shape of distilled and deionized water bolus.

Fig.4 shows the average surface depth and average inner depth of heat delivered to T3 malignant tissues. A 0.915 GHz antenna was coupled with various shapes of water boluses and able to destroy T3 malignant tissues. The required surface depth and inner depth for T3 malignant tissues are 35 mm and 95 mm, respectively. The graph shows that all shapes and types of water boluses achieved the required surface depth of T3 malignant tissues. However, for average inner depth, all shapes and types of water boluses reached the required inner depth, except the antenna with rectangular deionized water bolus does not meet the required inner depth.

DISCUSSION

Table II in the first column, shows sample of SAR generated by the applicator T1 with and without water bolus. The antenna's heat is distributed to both malignant tissues and healthy tissue. Integrating a circular microstrip patch antenna with various geometries of distilled and deionized water bolus reduced undesired hotspot. The duration to destroy malignant tissues is around 2 hours to 3 hours. The circular shape antenna with a rectangular shape of deionized water bolus demonstrates that the heat can penetrate to 73 mm which meet the required inner depth at 68 mm for the T1 applicator. In addition, the same antenna with a circular shape of distilled water bolus demonstrated the shortest time duration using antenna with water bolus which took around 2.11 hours and heat can penetrate maximum up to 80 mm for destroying malignant tissues when compared to the other three shapes of water bolus. Deionized rectangular water bolus produced less unwanted hotspots compared to other shapes within 2.33 hours. Construction of T1 Applicator and water boluses need to be improved to optimize the antenna and enhance SAR performance.

Table II, in the second column shows the SAR produced by the T2 applicator. The antenna emits heat that concentrates on the region of cancerous tissues. Heat evenly spreads throughout the malignant tissues. The best results are performed using a circular shape antenna integrated with a rectangular distilled water bolus, which produced less undesired hotspots than other shapes of water bolus. The time to destroy malignant tissues is approximately 0.6 hours to 1.5 hours. The cone shape of deionized and distilled water bolus, as well as the circular shape of deionized water bolus, achieve a maximum penetration depth of 73 mm.

Table II in the third column, shows the SAR generated by the T3 applicator. The antenna emits heat that spreads to malignant tissue. Heat is explicitly directed at the affected area of breast tissues. The most optimal outcome is achieved with a rectangular distilled water bolus capable of penetrating malignant tissues up to a depth of 108 mm. The time required to destroy malignant tissues is less than 0.5 hours. The T3 applicator exhibits the lowest occurrence of unwanted hotspots within the breast phantom compared to the other two applicators.

Table III in the first row and fourth row, shows results of an applicator T1, a 2.45 GHz antenna paired with various shapes of deionized and distilled water bolus and placed on the surface of the breast phantom. Some modifications for the antenna are made to deliver heat to the malignant tissues. The modifications include some changes, such as the position of the antenna was reversed, the antenna moving 80 mm to the upper part of the breast phantom, and placed 45 from the breast phantom. The modification enables heat to move

towards the malignant tissues. The required surface depth and inner depth for TI malignant tissues are 53 mm and 68 mm, respectively. However, the applicator for T1 creates significant undesired heating, especially at the front side of the breast phantom. Excessive heat can also be seen in Table III, where the heat is produced at 22 mm, 23 mm and 25 mm from the required surface depth of 53 mm.

CONCLUSION

In conclusion, an antenna integrated with distilled and deionized water bolus could transfer electromagnetic waves to the breast phantom and distribute the heat uniformly in the breast phantom. The coupling between the applicator and the water bolus minimizes undesired areas of high temperature in the breast model, whereas applying heat with the antenna without the water bolus leads to significant and undesirable regions of high temperature within the breast model. Additionally, water boluses not only cool the surface area of the breast phantom but also retain the focus position distance on the treated areas. T1 applicator showed good SAR results when the antenna was integrated with two shapes of distilled and deionized water bolus which is in rectangular and circular shape. The T2 applicator yielded optimal SAR performance when a circular antenna was paired with two shapes of water bolus either using deionized circular or deionized cone water bolus. There is a significant decrease of undesired areas of excessive heat around the treated regions.

Meanwhile, applicator T3 has demonstrated three shapes of water bolus such as circular, sphere and cone distilled and deionized water bolus can effectively reach the desired focus position distance within the malignant tissues. Electromagnetics properties that influence SAR including antenna characteristics such as the frequency, sizes, shapes and feedline along with the addition of the water bolus which significantly influence the Specific Absorption Rate (SAR), focus position distance and penetration depth in the hyperthermia treatment. We can see from the results shown in Table II and Table III, where heat delivered with water bolus reduced unwanted hotspots in the surrounding healthy tissues and focuses more to the target region. Water bolus helps to alleviate undesired significant heating in healthy tissues by providing cooling and altering SAR distribution. The different sizes and shapes of water bolus influenced the heat delivered to T1, T2 and T3 malignant tissues. The shape of the water bolus is manipulated in order to provide adequate heat to the malignant tissues while minimizing the presence of undesirable hotspots. From the experiment, the estimated time required to eradicate malignant tissues of T1, T2 and T3 is around 0.1 hour to 3 hours. Further research on hyperthermia treatment is required to improve the performance of circular antenna to reduce undesired heat for applicator T1. Water boluses of different shapes and antenna frequencies able to destroy different sizes of malignant tissues. Increasing the duration of hyperthermia therapy will enhance the SAR performance and influence the penetration depth.

ACKNOWLEDGEMENT

The author would like to thank Universiti Malaysia Sarawak (UNIMAS) for research facilities provided and for supporting this research. The author would also like to thank the College of Engineering, Electrical Engineering Studies UiTM Sarawak, for their continuous support throughout this research.

REFERENCES

1. Tan KF, Adam F, Hami R, Shariff NM, Mujar NMM. Review of breast cancer in young women. Malaysian J Med Heal Sci. 2020;16(4):370–8.
2. Bray F, Laversanne M, Sung H, Ferlay J, Siegel RL, Soerjomataram I, et al. Global cancer statistics 2022: GLOBOCAN estimates of incidence and mortality worldwide for 36 cancers in 185 countries. CA Cancer J Clin. 2024;74(3):229–63. doi.org/10.3322/caac.21834
3. Wilkinson L, Gathani T. Understanding breast cancer as a global health concern. Br J Radiol. 2022;95(1130):7–9. doi.org/10.1259/bjr.20211033
4. Ling WV, Lias K, Buniyamin N, Basri HM, Ahmad Narihan MZ. SAR distribution of non-invasive hyperthermia with microstrip applicators on different breast cancer stages. Indones J Electr Eng Comput Sci. 2021;22(1):232–40. doi.org/10.11591/ijeecs.v22.i1.pp232-240
5. Kok HP, Cressman ENK, Ceelen W, Brace CL, Ivkov R, Grьll H, et al. Heating technology for malignant tumors: a review. Int J Hyperth [Internet]. 2020;37(1):711–41. Available from:doi.org/10.1080/02656736.2020.1779357
6. Yi GY, Kim MJ, Kim HI, Park J, Baek SH. Hyperthermia Treatment as a Promising Anti-Cancer Strategy: Therapeutic Targets, Perspective Mechanisms and Synergistic Combinations in Experimental Approaches. Antioxidants. 2022;11(4). doi.org/10.3390/antiox11040625
7. Hassanmm, Lias K, Buniyamin N, Naimullah BSS, Jobli AT. SAR Performance of Rectangular Microstrip Antenna for Breast Cancer Hyperthermia Treatment with Different Period of Treatment Procedure. J Phys Conf Ser. 2021;2071(1):012048. doi.org/10.1088/1742-6596/2071/1/012048
8. Habash RWY. Therapeutic hyperthermia [Internet]. 1st ed. Vol. 157, Handbook of Clinical Neurology. Elsevier B.V.; 2018. 853–868 p. doi.org/10.1016/B978-0-444-64074-1.00053-7
9. Ni L-P, Sun H-T, Wang P, Wang J, Zhou J-H, Cao R-Q, et al. Hyperthermia enhances the efficacy of chemotherapeutic drugs in heat-sensitive cells through interfering with DNA damage repair.

Ann Transl Med. 2022;10(8):463–463. doi.org/10.21037/atm-22-955
10. Stauffer PR, Rodrigues DB, Sinahon R, Sbarro L, Beckhoff V, Hurwitz MD. Using a conformal water bolus to adjust heating patterns of microwave waveguide applicators. Prog Biomed Opt Imaging - Proc SPIE. 2017;10066. doi.org/10.1117/12.2252208
11. Mendez HFG, Pantoja JJ, Arango MAP. Hyperthermia study in cancer treatment. 2018 Int Appl Comput Electromagn Soc Symp Denver, ACES-Denver 2018. 2018;1–2. doi.org/10.23919/ROPACES.2018.8364294
12. Olufadi YB, Maina I, Adegboye OA, Ireti Fasiku A. Comparative Analysis of the Effect of Different Substrates Materials on Microstrip Patch Antenna Operating at 3.6 GHz. Proc IEEE Int Conf Prop Appl Dielectr Mater. 2021;2021-July(Icpadm):81–4. doi.org/10.1109/ICPADM49635.2021.9493967
13. Arora G, Maman P, Sharma A, Verma N, Puri V. Systemic overview of microstrip patch Antenna's for different biomedical applications. Adv Pharm Bull. 2021;11(3):439–49. doi.org/10.34172/apb.2021.051
14. Hassanmm, Lias K, Buniyamin N, Narihan MZA, Naimullah BSS, Ispawi DI. SAR Analysis Using Various Substrates of Microstrip Antenna for Breast Cancer Hyperthermia Treatment. J Phys Conf Ser. 2023;2622(1). doi.org/10.1088/1742-6596/2622/1/012006
15. Rosella Gaffoglio, Marco Righero, Giorgio Giordanengo MZ and GV. Fast Optimization of Temperature Focusing in hyperthermia treatment os sub superficial tumors.pdf. IEEE J Electromagn RF Microwaves Med Biol. 2020; doi.org/10.1109/JERM.2020.3043383
16. Lias K, Buniyamin N, Narihan MZA. Simulation study of an EBG-M applicator towards non-invasive breast hyperthermia cancer procedure. J Teknol. 2016;78(5–6):75–81. doi.org/10.11113/jt.v78.8641
17. Miaskowski A, Gas P, Szczygieł M. Optimization of SAR coefficient for dipole antennas array with regard to local hyperthermia. 2018 Appl Electromagn Mod Tech Med PTZE 2018. 2018;163–6.
18. Pathak PP, Tripathi H, Kumar V. Specific Absorption Rate Calculation and Rate of Temperature Change in Tissues Due to Radio Antenna. Int Trans Appl Sci. 2010;2(4):739–47.